

# Effects of Al<sub>2</sub>O<sub>3</sub> Nanopowders on the Wear Behavior of NiTi Shape Memory Alloys

Y. ŞAHİN<sup>1</sup> and K. EMRE ÖKSÜZ<sup>2,3</sup>

1.—Department of Manufacturing Engineering, Gazi University, Besevler, 06500 Ankara, Turkey. 2.—Department of Metallurgical Materials Engineering, Cumhuriyet University, 58140 Sivas, Turkey. 3.—e-mail: kerimemreoksuz@gmail.com

TiNi shape memory alloy and its composite using  $\delta$ -Al<sub>2</sub>O<sub>3</sub> nanosize particles were prepared by the powder metallurgy method, and some mechanical properties like hardness, wear, and corrosion behavior were investigated. The experimental results exhibited that the lower wear rate was obtained for the nano-Al<sub>2</sub>O<sub>3</sub>-reinforced Ti alloy composite due to increased hardness, but the wear rate increased considerably with increasing the load over 25 N for Ti alloy. However, the best corrosion resistance was obtained for the base alloy, which is very important for implant applications.

## INTRODUCTION

Titanium and its alloys are widely employed for implant materials in the medical and dental areas due to their superior biocompatibility, corrosion resistance, and specific strength compared with other metallic implant materials.<sup>1</sup> The mechanical properties of pure Ti can be improved to produce titanium-nickel (NiTi) alloys by controlling the synthesis condition. TiNi shape memory alloys (SMAs) also offer a combination of novel properties such as the shape memory effect, super elasticity, biocompatibility, and high damping capacity, which enable them to be widely used in numerous applications, especially for biomedical engineering and microelectromechanical systems (MEMS).<sup>2,3</sup> TiNi alloys have been fabricated using various methods like metal injection molding, hot isostatic pressing, combustion synthesis, and spark plasma sintering. Solid-state processes are generally used to obtain the best mechanical properties in titanium-based composites. These processes exhibit excellent finished performance due to the ability to obtain uniform distribution of reinforcement and near-net shape formability.<sup>4</sup>

The progress in manufacturing and characterization of TiNi alloys has been reported by a number of researchers. Ye et al.<sup>5</sup> studied that TiNi-based composites, reinforced, respectively, with TiC and TiN were developed by using a sintering process. It was demonstrated that the composite exhibited an enhanced wear resistance with a considerable level.

Dunand et al.<sup>6</sup> investigated a TiNi-based composite with 20 vol.% TiC hard particle. They found that the TiC particles mainly affected the phase transformation temperature but did not influence the shape memory effect of the TiNi matrix. Ye et al.<sup>7</sup> studied that the wear resistance increased with an increase in the content of TiC particles, and among the TiC/TiNi specimens tested, the optimal fraction of TiC particles was 60%. The wear resistance of 60% TiC/TiNi composite was on three orders of magnitude higher than that of the 304 steel and on one order of magnitude higher than that of the TiNi alloys. However, TiNi alloy exhibited a wear resistance that was two orders of magnitude higher than that of stainless steel 304 under low loads with cooled disk.<sup>8</sup> Effects of the hot isostatic pressing (HIP) treatment on the reduction of pores in the TiC/TiNi and TiN/TiNi composites were studied.<sup>9</sup> Luo et al.<sup>10</sup> showed some improvements in the wear resistance of TiC/TiNi composite. Li<sup>11</sup> studied the sliding wear behavior of Ti–50.3 at.% Ni alloy and compared to 2Cr13 steel. TiNi alloy exhibited a much higher resistance to wear although it had a lower hardness compared to the 2Cr13 steel.<sup>12,13</sup> Liang et al.<sup>14</sup> investigated the wear behavior of TiNi alloy during sliding wear, impact abrasion and sandblasting erosion. They noticed a strong correspondence between the wear resistance and the recoverable strain resulting from the pseudoelasticity (PE). Li and Ma<sup>15</sup> reported the wear resistance of the alloy benefits from its PE.

Li<sup>16</sup> demonstrated that the TiNi matrix composites could be further enhanced by both the HIP

treatment and addition of nanoparticles that improved mechanical properties of the matrix. Ninomi<sup>4</sup> reported that V and Al free alloys were developed.<sup>3</sup> Arciniegas et al.<sup>17</sup> studied that five TiNi alloys were prepared with compositions varying from 49 at.% to 51 at.% Ni, austenized at 800°C for 10 min, quenched in water, and annealed at 500°C for 1 h before air cooling. On  $\beta$ -phase alloys, the wear behavior was influenced by the presence of semicoherent precipitates as well as its high capacity of transformation, and then, by decreasing the damage mechanisms while in martensite-phase alloys, it was conditioned by the reorientation and/or retransformation of the existent plates. Della-Corte<sup>3</sup> investigated an intermetallic nickel-titanium alloy, 60NiTi, which offered a broad combination of physical properties. The optimal composition was from Ti-55wt.%Ni to Ti-56.5wt.%Ni.<sup>18,19</sup>

The literature reviews have demonstrated that equiatomic TiNi alloy exhibits high mechanical and wear resistance.<sup>1-4,8-10,15-17</sup> Some attempts were made previously to develop TiNi-matrix composites.<sup>5,6,9,12</sup> However, a very limited study on the nanoscale powders was used for manufacturing TiNi alloys.<sup>10,12</sup> The aim of this work is to produce NiTi alloys and its metal matrix composites (MMCs) using nano- $\delta$ -Al<sub>2</sub>O<sub>3</sub> particles with the powder metallurgy (PM) route and to study the mechanical properties (hardness, corrosion, and wear) of NiTi alloy SMAs to evaluate their short- and long-term behavior as structural biomaterials.

## EXPERIMENTAL PROCEDURE

Commercially pure Ti powders about 325 mesh ( $\sim 45 \mu\text{m}$ ) and Ni powders (99.9% purity) about 325 mesh ( $\sim 45 \mu\text{m}$ ) were used to fabricate NiTi alloy by the PM route in this study. Nanosized  $\delta$ -alumina was selected to manufacture NiTi-based metal matrix composites. They were both obtained from Alfa Aesar (Ward Hill, MA). To produce Al<sub>2</sub>O<sub>3</sub>-NiTi-based composites, Ti powders with an average particle size of  $45 \mu\text{m}$  with 99.5% purity were chosen while nano-Al<sub>2</sub>O<sub>3</sub> particles measuring 20 nm in size were used as the reinforcements. The powder mixture with the nominal composition of Ti-50 at.% Ni was blended. TiNi and Al<sub>2</sub>O<sub>3</sub> particle-reinforced composites were also fabricated using the same route. The mixed powders were cold pressed into pin specimens under a pressure of 650 MPa. These specimens were sintered at 1150°C in a tube-type furnace in an argon gas control for 3 h. Hereafter, it is denoted as pure titanium, Ti<sub>50</sub>Ni<sub>50</sub> alloy, Ti-Ni<sub>45</sub>-5Al<sub>2</sub>O<sub>3</sub> nanocomposite, and Ti-Ni<sub>40</sub>-10Al<sub>2</sub>O<sub>3</sub> nanocomposite (Table I). The hardness of the composite and its alloy were measured by Vickers hardness (VHN) method and the mean of at least five readings was taken.

The wear resistance of the specimens was evaluated using a pin-on-disk tribometer by measuring the weight loss after sliding over 2100 m at a fixed speed. Corrosion tests were carried out in H<sub>2</sub>SO<sub>4</sub> solution,

**Table I. Composition of intermetallic composites**

| Samples                                                              | Compositions (wt.%)                           | Code                              |
|----------------------------------------------------------------------|-----------------------------------------------|-----------------------------------|
| Pure Ti                                                              | 100                                           | Matrix                            |
| Ti <sub>50</sub> +Ni <sub>50</sub>                                   | Ti%50+Ni%50                                   | Ti <sub>50</sub> Ni <sub>50</sub> |
| Ti <sub>50</sub> +Ni <sub>45</sub> +5Al <sub>2</sub> O <sub>3</sub>  | Ti%50+Ni%45+%5Al <sub>2</sub> O <sub>3</sub>  | Ti-Ni <sub>45</sub> -5nano        |
| Ti <sub>50</sub> +Ni <sub>40</sub> +10Al <sub>2</sub> O <sub>3</sub> | Ti%50+Ni%40+%10Al <sub>2</sub> O <sub>3</sub> | Ti-Ni <sub>40</sub> -10nano       |

pH-1.50 solution at room temperature, and 45°C. The samples were placed in H<sub>2</sub>SO<sub>4</sub> of pH 1.5 for 3 h.

## RESULTS AND DISCUSSION

### Microstructure of TiNi Alloy and Its Composite

Figure 1a shows the scanning electron microscope (SEM) micrograph of TiNi alloy containing 50 wt.% of each one, sintered at 1150°C for 3 h. The figure shows some pores in the microstructure. The average value of pore sizes is about 20  $\mu\text{m}$  to 30  $\mu\text{m}$ . The structure is composed of two regions, one is gray colored (Ti) and the other part is shown with black one (Ni). Figure 1b shows the SEM image of Ti-Ni<sub>45</sub> alloy reinforced with a 5 wt.% Al<sub>2</sub>O<sub>3</sub> particle measuring 20 nm in size. It can be seen that the Al<sub>2</sub>O<sub>3</sub> powders cannot be visible in this photograph due to the possibility of dissolution in Ti or Ni and its fine grain size. Figure 1 also indicates that the level of porosity in Ti<sub>50</sub>+Ni<sub>45</sub>+5wt.%Al<sub>2</sub>O<sub>3</sub> structure seems to be higher than that of the Ti<sub>50</sub>Ni<sub>50</sub> composite.

### Density Measurement and Hardness Tests

The density of the composites was obtained by weighing small pieces cut from the composites disk first in air and water, and then by calculating the density by Archimedeian method (Fig. 2a). The porosities are about 12.87, 28.04, and 29.30 for Ti, Ti<sub>50</sub>Ni<sub>50</sub>, and its composite, respectively. The hardness of the composites was determined after polishing to a 3  $\mu\text{m}$  finish. The VHN value was measured at a load of 0.25 kg-f for the matrix and the composites, taking the mean of at least four tests. The variation of hardness of the composites is shown in Fig. 2b. This figure indicated that the hardness of the MMCs increased with increasing the content of particles up to 5 wt.% and then decreased thereafter.<sup>9,16</sup> The hardness for pure Ti and its composite are about 517 VHN, 666 VHN, 882 VHN, and 590 VHN for the matrix, Ti<sub>50</sub>Ni<sub>50</sub> alloy, Ti<sub>50</sub>-Ni<sub>45</sub>-5 nanocomposite, and Ti-Ni<sub>40</sub>-5 nanocomposites, respectively.

### Wear Behavior of NiTi Alloy/Al<sub>2</sub>O<sub>3</sub> Reinforced Composite

The average volumetric wear rate of NiTi-Al<sub>2</sub>O<sub>3</sub>-reinforced composites is illustrated graphically in

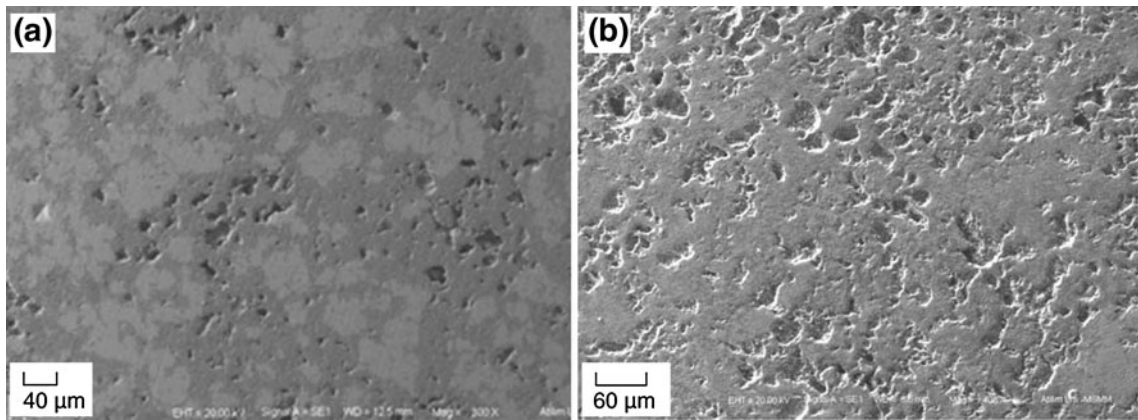


Fig. 1. (a) Microstructure of Ti<sub>50</sub>Ni<sub>50</sub> alloy sintered at 1150°C for 3 h and (b) Ti<sub>50</sub>Ni<sub>45</sub>+5wt.%Al<sub>2</sub>O<sub>3</sub>-reinforced nanocomposite.

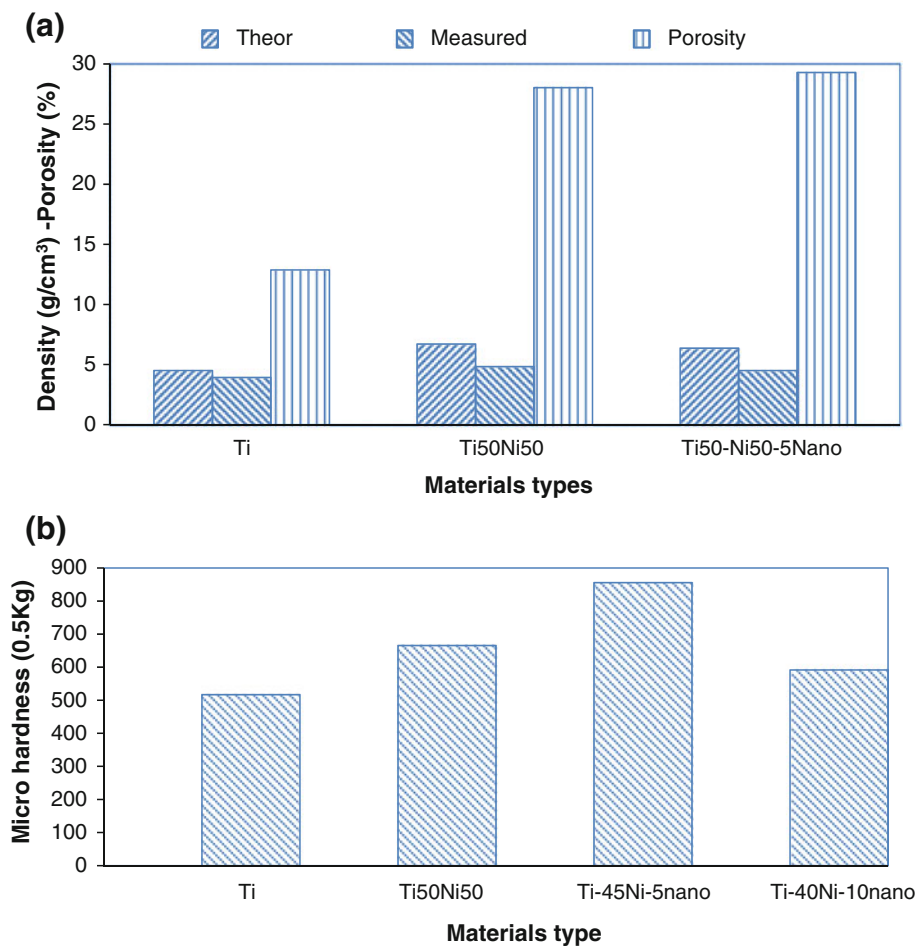


Fig. 2. (a) Density of TiNi alloy and its nanocomposite. (b) Hardness of TiNi alloy and its composite.

Fig. 3a as a function of different loads. It is found that the wear rate of the composites increased with all applied loads for tested materials. It is evident from the figure that the composite had lower wear rates than that of the Ti matrix at whole loads. However, first there was a slight increasing trend in the wear of the matrix alloy, and then there was a

significant increase in the wear of the base alloy after 25 N load although its microstructure showed no porosity.

In the composites, there was a stable behavior under 10 N and 25 N loads. Over 25 N loads, slight increases in wear rate of the composite were observed. One reason is that nanosized alumina

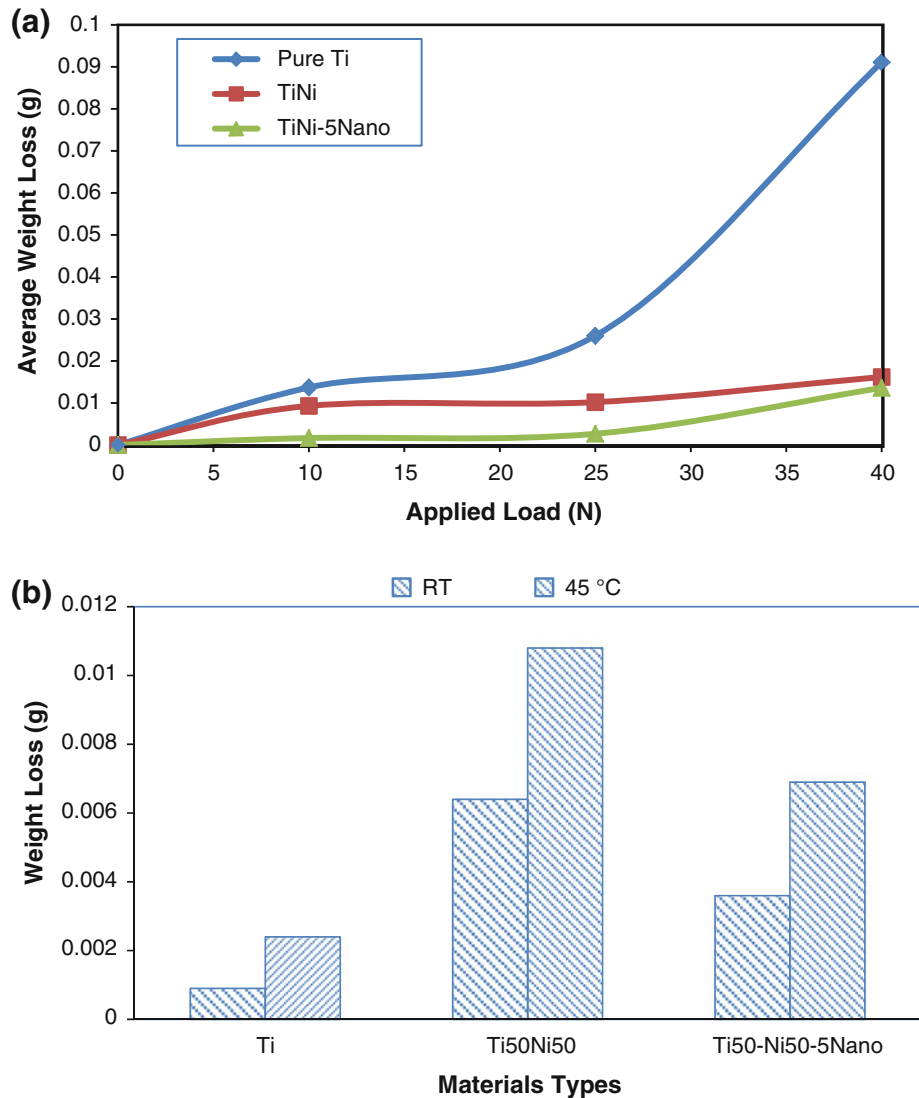


Fig. 3. (a) Variation of average volumetric wear rate as a function of applied loads for 10 wt.%  $\text{Al}_2\text{O}_3$ -reinforced composite and its matrix alloy. (b) Corrosion test results on the tested samples.

particles prevent the movement of dislocations in Ti matrix through a dispersion-strengthening mechanism. In addition, 5 wt.%- $\text{Al}_2\text{O}_3$  particle-reinforced MMCs demonstrated lower wear than that of 10 wt.%- $\text{Al}_2\text{O}_3$  particle-reinforced MMCs. This indicated the critical weight fraction of particles in the TiNi alloy. A similar observation was obtained in the previous work.<sup>10</sup> The wear resistance of TiNi benefited from its special deformation property—PE, which originated from a reversible phase transformation between a B19' phase and a B2 phase.<sup>8</sup> Corrosion tests were carried out in  $\text{H}_2\text{SO}_4$  with pH 1.50 solution at 3 h. The test results are represented in Fig. 3b. It is clear from the result that pure Ti showed the best corrosion resistance, followed by nanobased composites, but  $\text{Ti}_{50}\text{Ni}_{50}$  alloy indicated the highest corrosion rate due to lower sintered density, which could be correlated with higher porosity level.

## CONCLUSIONS

The effect of nano- $\text{Al}_2\text{O}_3$  particles on the wear and mechanical properties of TiNi alloy was investigated. The microhardness of NiTi alloy improved with the introduction of  $\text{Al}_2\text{O}_3$  particles. The volumetric wear rates of the NiTi alloy and its composites increased with increasing the load. The change was very small for the composite but very large for the base alloy over 25 N loads. Among the tested samples, the best corrosion resistance was obtained for the Ti alloy because of lower porosity level.

## OPEN ACCESS

This article is distributed under the terms of the Creative Commons Attribution License which permits any use, distribution, and reproduction in any medium, provided the original author(s) and the source are credited.

## REFERENCES

1. L.G. Machado and M.A. Savi, *Braz. J. Med. Biol. Res.* 36, 683 (2003).
2. Y.Q. Fu, H.S. Du, V.M. Huang, S. Zhang, and M. Hu, *Sens. Actuators* 112, 395 (2004).
3. C. DellaCorte, "Nickel-Titanium Alloys: Corrosion Proof Alloys for Space Bearing, Components and Mechanism Applications" (Paper presented at the 40th Aerospace Mechanisms Symposium, NASA, 12–14 May, 2010).
4. M. Ninomi, *Mater. Sci. Eng. A* 243, 231 (1998).
5. H. Ye, R. Liu, D.Y. Li, and R. Eadie, *Scripta Mater.* 41, 1039 (1998).
6. D.C. Dunand, D. Mari, M.A.M. Bourke, and J.A. Roberts, *Metall. Mater. Trans. A* 27A, 183 (1996).
7. H. Ye, R. Liu, D.Y. Li, and R. Eadie, *Compos. Sci. Technol.* 6, 987 (2001).
8. R. Liu and D.Y. Li, *Metall. Mater. Trans. A* 31, 2773 (2000).
9. H.Z. Ye, D.Y. Li, and R.L. Eadie, *Mater. Sci. Eng. A* 329–331, 750 (2002).
10. Y.C. Luo, R. Liu, and D.Y. Li, *Mater. Sci. Eng. A* 329–331, 768 (2002).
11. D.Y. Li, *Wear* 225–229, 777 (1999).
12. D.Y. Li and Y. Luo, *J. Mater. Sci. Lett.* 20, 2249 (2002).
13. Y. Luo and D.Y. Li, *J. Mater. Sci.* 36, 4695 (2001).
14. Y.N. Liang, S.Z. Li, Y.B. Jin, W. Jin, and S. Li, *Wear* 198, 236 (1996).
15. D.Y. Li and X. Ma, *Mater. Sci. Technol.* 17, 15 (2001).
16. D.Y. Li, *Wear* 255, 617 (2003).
17. M. Arciniegas, J. Casals, J.M. Manero, J. Peña, and F.J. Gil, *J. Alloy. Compd.* 460, 213 (2008).
18. T. Zhang and D.Y. Li, *Mater. Sci. Eng. A* 14, 293 (2000).
19. H.C. Lin, H.M. Liao, J.L. He, K.M. Lin, and K.C. Chen, *Metall. Mater. Trans. A* 28A, 1871 (1997).